LANGMUIR

pubs.acs.org/Langmuir Article

Covalent and Hydrogen Bonding in Adsorption of Alanine Molecules on Si(111)7×7

L. Zhang, H. Farkhondeh, F. R. Rahsepar, A. Chatterjee, and K. T. Leung*

Cite This: *Langmuir* 2021, 37, 5540−5547 Read Online

ACCESS | Metrics & More | Article Recommendations

ABSTRACT: Molecular adsorption bonding configurations and specific interfacial chemistry of alanine on Si(111)7×7 have been determined by combining the results from scanning tunneling microscopy (STM) and X-ray photoelectron spectroscopy (XPS) with ab initio calculations based on the density functional theory (DFT). XPS spectra of the N 1s region show that alanine molecules bind to the 7×7 surface by N−Si covalent bonding, while STM imaging reveals that such N−H dissociative adsorption of alanine occurs on an adjacent Si adatom-restatom pair, with the dehydrogenated alanine moiety and dissociated H atom occupying the Si adatom and restatom sites, respectively. At a sample bias above +2 V, the dehydrogenated alanine appears as a bright round protrusion, slightly off-center from a Si adatom site and leaning toward the opposite Si adatom across the dimer wall. The off-center character can be attributed to an electrostatic attraction between the electron-rich carbonyl O of the dehydrogenated alanine and electron-deficient nearest Si adatom across the dimer wall. Our DFT calculation also shows that the monodentate O−Si bonding configuration resulting from O−H dissociative adsorption is more thermodynamically favorable than the experimentally observed N−Si bonding configuration, suggesting that the interfacial dissociative adsorption reaction is a kinetically controlled rather than a thermodynamically driven process. Alanine molecules in the second adlayer (transitional layer) are found to attach to those in the first adlayer (interfacial layer) by N···HO hydrogen bonding, as supported by the presence of the N 1s feature at 401.0 eV. An alanine molecule H-bonded to a dehydrogenated alanine in the first adlayer has also been observed in STM as a brighter and larger protrusion close to the expected location of the free OH group in the dehydrogenated first-adlayer alanine. No thick zwitterionic alanine film can be obtained at room temperature possibly due to steric constraint caused by the methyl group.

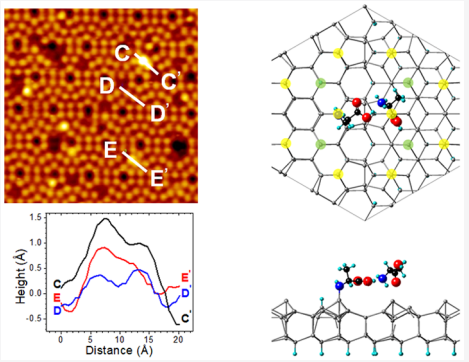

INTRODUCTION

As the well-developed electronics industry has traditionally relied on the metal−semiconductor, oxide-semiconductor, and semiconductor-semiconductor interfaces (i.e., the inorganic to semiconductor interfaces), integration of biomolecules with semiconductors and, particularly, exploitation of the bio/organic molecules to semiconductor interfaces have opened up new opportunities in the application of biosensors, bioelectronics and biocompatible materials.[1,2] Biomolecules such as peptides, proteins, and nucleic acids are made up of smaller building blocks (amino acids and nucleobases), which contain multiple functional groups. The broad range of functional groups available in biomolecules provides great versatility and flexibility over inorganic materials. Even the smallest amino acid molecules such as glycine ($NH_2C_\alpha H_2COOH$) and alanine [$NH_2C_\alpha H(CH_3)COOH$], each of which contains only two functional groups, have exhibited significant chemical, structural and chiral complexities, especially when they adsorb on solid surfaces.[3] Depending on the nature of the adsorbate and the substrate surface and on the coverage and temperature, various types of adsorption bonding configurations (mono-, bi-, and tridentate) could lead to different surface reactions (such as dissociation, cycloaddition, dative bond mediated reactions) at the interface. Resolving the complexities of the adsorption and growth of small biomolecules on solid surfaces therefore requires multiple analytical techniques. Surface-sensitive techniques, such as X-ray photoelectron spectroscopy (XPS), surface vibrational spectroscopy, and X-ray absorption spectroscopy, provide chemical composition and structural bonding information averaged over a small sampling area. On the other hand, scanning tunneling microscopy (STM) provides direct imaging of the local density of states at atomic resolution, therefore furnishing unique site-specific information. Together, these techniques provide more comprehensive information and better understanding of biomolecular adsorption and surface processes at the atomic level.

Received: January 29, 2021
Revised: April 7, 2021
Published: April 21, 2021

https://doi.org/10.1021/acs.langmuir.1c00283
Langmuir 2021, 37, 5540−5547

We have studied the adsorption bonding configurations of glycine on Si(111)7×7 by using a three-pronged approach of combining XPS and STM data with density functional theory (DFT) calculations.[4,5] A glycine molecule is found to undergo N−H dissociative adsorption, with its amino group reacted with a Si adatom-restatom pair of the 7×7 surface through N−Si and H−Si covalent bonding. Glycine molecules in the second adlayer (transitional adlayer) could bind to those in the first adlayer by N···HO hydrogen bonding, and zwitterionic multilayer formation follows upon further deposition. When a H atom bonded to the alpha C in a glycine molecule is replaced by a methyl group, the resulting alanine molecule ($NH_2C_\alpha H(CH_3)COOH$), as the second smallest amino acid, offers a unique testing ground for studying the methylation effects on interfacial molecular bonding, chirality and film growth. Although the methyl group is not chemically reactive, it increases the size and complexity of the molecular structure of the amino acid, potentially introducing steric constraint, all of which could affect how alanine bonds to the surface and how it interacts with one another during film growth. Adsorption of alanine, cysteine, aspartic acid, proline, glutamic acid and methionine on single crystalline metal surfaces [Cu(110), Au(111), Ag(100), Ni(100)] and on nonreactive Si(111)-$\sqrt{3}\times\sqrt{3}$-Ag surface, have been extensively studied by using XPS, reflection−absorption infrared spectroscopy, temperature-programmed desorption, low-energy electron diffraction, and STM.[6−18] In particular, a comprehensive adsorption phase diagram of alanine on Cu(110) has been reported to include four alaninate ($NH_2C_\alpha H(CH_3)COO^-$) phases depending on the coverage and substrate temperature.[9] At room temperature, individual alanine molecules were found to bond tridentately to Cu(110) at low coverage through both carboxylate O atoms and the amino N atom, following deprotonation of the carboxylic acid group. Interestingly, the tridentate bonding was so weak that the alaninate adspecies was highly mobile on terraces leading to the observed streaks in the STM image. The absence of strong adsorbate−substrate interactions has accentuated intermolecular interactions that facilitate self-assembly of alaninate observed at higher coverages.[9] There are only a few studies on alanine adsorption on semiconductor surfaces. A bidentate configuration through two carboxylate O atoms has been proposed for alanine adsorption on ZnO($10\bar{1}0$),[19] while a monodentate configuration through the hydroxyl O atom following O−H dissociation on Ge(100)2×1 was obtained by using DFT calculation and found to be both kinetically and thermodynamically favorable.[20] Although the zwitterionic form is the most stable form in the solid state for amino acids, no zwitterionic multilayers have been reported for alanine at 300 K regardless of the substrate, in marked contrast to glycine and other amino acids.[4,21−23] Formation of zwitterionic alanine multilayers has, however, been observed on Pd(111) and ZnO($10\bar{1}0$) at low temperature (≤250 K).[7,19]

Here, we study alanine adsorption on Si(111)7×7 by combining the chemical-state information provided by XPS with the local density of state (LDOS) information obtained by STM. We also determine the adsorption structures (and energies) of several plausible molecular bonding configurations by DFT calculations and compare the calculated structures with those derived experimentally. Not only does the Si(111)7×7 surface provide various geometrically and electronically specific reactive sites, therefore offering different adsorption possibilities, there is also a wealth of information on the adsorption of atoms (e.g., H and O) and small molecules (e.g., NH_3 and H_2O) on this surface. In the dimer-adatom-stacking fault model, the Si(111)7×7 unit cell consists of a faulted and an unfaulted triangular half unit cells, with 19 dangling bonds distributed over 12 positively charged adatom sites, 6 negatively charged restatom sites, and 1 corner hole site.[24−26] The partial charge polarity in an adjacent adatom-restatom pair is believed to induce chemical adsorption of organic molecules via dissociation, and [2 + 2]- or [4 + 2]-like addition pathways.[27] In STM LDOS imaging, both adatoms and restatoms can be observed in filled-state images, while only adatoms are visible in empty-state images. In comparison to metal single-crystal surfaces and Si(100)2×1, the relatively large surface corrugation and wide separation among adatoms and restatoms on Si(111)7×7 offer an opportunity to determine bonding configuration of a single adsorbed molecule from their LDOS dependence on the adsorption location and sample bias and from the resulting change in appearance in the adspecies and adjacent Si adatoms and restatoms. In the present work, STM imaging of alanine adsorption on Si(111)7×7 reveals bright round protrusions on top of the Si adatoms, but slightly off-center gravitating toward the opposite Si adatoms across the dimer wall. In addition, the presence of restatoms appears to be obscured near these bright protrusions. Given the XPS results that suggest bonding of alanine to the 7×7 surface through the N−Si bond following N−H bond dissociative adsorption, we conclude that an alanine molecule reacts with an adjacent adatom−restatom pair, with the dehydrogenated alanine and dissociated H atom occupying the adatom and the restatom sites, respectively. The minor but discernible off-center shift of the dehydrogenated alanine toward the opposite adatom across the dimer wall suggests an electrostatic attraction between the electron-rich carbonyl O atom and electron-deficient Si adatom. The position of the dehydrogenated alanine and the appearance of the surrounding Si adatoms help to rule out a few other bonding configurations, despite being more thermodynamically stable in our DFT calculations, which suggests the importance of kinetically controlled adsorption pathways. While the bonding configuration of alanine on Si(111)7×7 and the presence of (N···HO) hydrogen-bonded alanine on the second adlayer are found to be similar to those of glycine on Si(111)7×7, thick zwitterionic film formation of alanine is not observed, though the presence of patchy alanine zwitterionic islands could not be ruled out, in marked contrast to glycine. The methyl group and its accompanied steric constraint could therefore play a key role in preventing incoming neutral alanine molecules from accumulation and growth into a thick film.

EXPERIMENTAL AND COMPUTATIONAL DETAILS

The experiments were performed in an ultrahigh vacuum five-chamber system (Omicron Nanotechnology Inc.) with a base pressure lower than 5×10^{-11} mbar, described in detail elsewhere.[4] The analysis chamber was equipped with an XPS spectrometer and a variable-temperature scanning probe microscope. The XPS spectrometer consisted of a SPHERA hemispherical electron analyzer with a 7-channeltron detector and a monochromatized Al Kα source (with 1486.7 eV photon energy). The STM system was operated in a constant current mode using an electrochemically etched W tip with a voltage bias applied on the sample held at room or low temperature. Single-side polished Si(111) chips (11×2 mm^2, 0.3 mm thick) with a resistivity of 5 mΩ cm (Virginia Semiconductors) were used as the substrates. After outgassing the Si substrate at 400 °C overnight

https://doi.org/10.1021/acs.langmuir.1c00283
Langmuir 2021, 37, 5540−5547

followed by flash-annealing at 1200 °C several times by direct-current heating, large terraces of the 7×7 surface reconstruction were observed with STM and no contaminants were detected with XPS. Powder of D-alanine (99% purity, Aldrich) was loaded into a water-cooled low-temperature organic effusion cell (Dr. Eberl MBE-Komponenten GmbH) mounted in a separate preparation chamber. The effusion cell was heated to 125 °C to effect deposition of alanine on the 7×7 surface held at room temperature. A quadrupole mass spectrometer was used in situ to confirm the molecular integrity of the alanine molecules (that were evaporated intact) and to provide quantitative estimate of the deposition rates at different temperatures. The deposition rate was ~0.04 monolayer (ML) per minute (where 1 ML is defined as the atomic density of unreconstructed Si(111) surface, that is, 7.8×10^{14} atom/cm^2), which was estimated by counting the number of adsorbed alanine molecules on a 7×7 surface in STM images. To prepare a thick alanine film, a higher cell temperature of 140 °C was used to provide a higher deposition rate of 0.2 ML/min. XPS spectra of the Si 2p, C 1s, N 1s, and O 1s regions were recorded with a pass energy of 20 eV, and the binding energy scale was calibrated with respect to Si $2p_{3/2}$ (at 99.3 eV). Alanine powder adhered to a carbon tape was also measured with XPS, and the sample charging problem was alleviated by using a charge neutralizer. The binding energy scale of the powder sample was calibrated by aligning the inert methyl C 1s feature of the powder with the film sample at 285.5 eV.

The first-principle density functional theory calculations were performed using the plane-wave based Vienna Ab initio Simulation Package (VASP, version 5.4) implemented on the Materials Exploration and Design Analysis (MedeA, version 2.19, Materials Design, Inc.) platform. The projector-augmented wave (PAW) method[28,29] was used to describe the electron−ion interactions, and the generalized gradient approximation (GGA) with the exchange correlation functional as defined by Perdew−Burke−Ernzerhof[30] was used to model the electron−electron exchange correlation energy. The dispersion energies were included in the calculations as implemented within the DFT-D2 formalism.[31] Conjugate gradient algorithm was employed to optimize the geometry of the atomic structure, and all Si atoms were completely relaxed until the forces on all the atoms were less than 0.01 eV/Å. The plane-wave expansion cutoff energy was set to 400 eV, and the surface Brillion zone was sampled at the Γ point with a k-point spacing of 0.5 Å^{-1}. The energy convergence of the self-consistent field was set to 1.0×10^{-5} eV, with a Methfessel−Paxton smearing of 0.2 eV. The dimer-adatom-stacking fault model was used to model the Si(111)7×7 substrate.[24] A periodic repeating slab consisting of two Si bilayers and a reconstructed adatom-restatom topmost layer (with a total number of 200 Si atoms) with a lattice constant of 5.41 Å and a vacuum gap of 10 Å was used to represent the Si(111)7×7 surface, and the bottom layer of the Si slab was terminated by 49 H atoms. To find the most stable adsorption configuration, an adsorbate alanine molecule was placed on various adsorption sites including the center and corner adatoms inside each faulted and unfaulted half unit cells and across the dimer wall. The positions of all atoms and molecules were relaxed during the DFT-D2 calculations. The adsorption energy, E_{ad}, is obtained with the formula $E_{ad} = E_{n(Ala)\text{-}Slab} - E_{Slab} - n(E_{Ala})$, where $E_{n(Ala)\text{-}Slab}$, E_{Slab} and E_{Ala} are the total energies of n alanine molecules adsorbed on the $Si_{200}H_{49}$ slab, the $Si_{200}H_{49}$ slab (as the model 7×7 surface), and the isolated alanine molecule, respectively.

RESULTS AND DISCUSSION

Figure 1 shows the O 1s, N 1s, and C 1s XPS spectra of alanine deposited on the Si(111)7×7 surface cumulatively with the effusion cell held at 125 °C for total exposure times of 60, 240, 480, and 960 s. These spectra are compared with those obtained for a "thick" alanine film deposited with the effusion cell held at 140 °C for 1920 s on the 7×7 surface, and those for alanine powder. Amino acid molecules exist in neutral form in the gaseous state, and in zwitterionic form in the solid state.

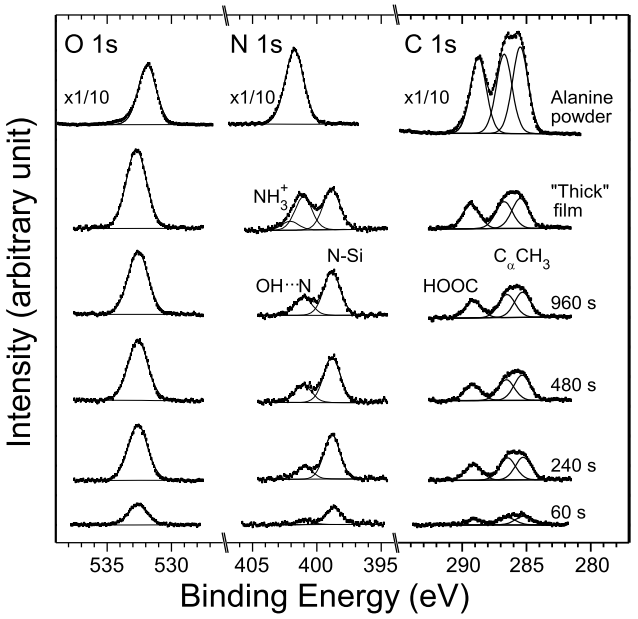

Figure 1. XPS spectra of the C 1s, N 1s, and O 1s regions of alanine deposited for total exposure times of 60, 240, 480, and 960 s with the effusion cell held at 125 °C, a "thick" alanine film deposited for 1920 s with the effusion cell set at 140 °C, all on Si(111)7×7 held at room temperature, and alanine powder.

Zwitterionation in the solid state can enhance dipole−dipole interaction and hydrogen bonding among neighboring molecules.[32] The zwitterionic powder sample exhibits a single N 1s peak at 401.7 eV corresponding to NH_3^+ and an O 1s peak at 531.9 eV corresponding to COO^- species, in good accord with those reported for alanine[7,19] and glycine zwitterions.[4,33,34] The corresponding C 1s spectrum consists of three components at 285.5, 286.7, and 288.7 eV, which can be assigned to the methyl (CH_3), α−C (C_α) and carboxylate (COO^-) species, respectively, in accord with the relative electronegativities of their neighboring atoms. The similar intensities found for these three C 1s components are in good agreement with their 1:1:1 stoichiometry.

The spectra of the thin films are found to be discernibly different from those of the powder sample, which suggests that alanine adopts adsorption structures other than the zwitterionic form in thin films. For the lowest coverage (0.04 ML, obtained with a 60 s exposure with the effusion cell held at 125 °C), the major N 1s component at 398.8 eV can be assigned to the N−Si covalent bonding feature, following dissociative adsorption of alanine through N−H bond cleavage.[35,36] The minor component at 401.0 eV is located between the protonated amino group NH_3^+ at 401.7 eV and neutral amino group NH_2 at 399.9 eV,[33] and it can therefore be attributed to the amino N involved in the N···HO hydrogen bonding. The hydrogen bonding is formed between the amino N of an alanine molecule in the second adlayer and the hydroxyl group of a dehydrogenated alanine in the first adlayer. Similar hydrogen bonding has also been found between several small prototypical biomolecules (glycine, glycylglycine, and adenine) and a glycine-functionalized Si(111)7×7 surface.[4,37] Indeed, intramolecular N···HO hydrogen bonding has also been reported for one of the two most stable conformers of alanine in the gaseous state, which leads to a N 1s binding energy 0.7 eV higher than that of a non-H-bonded conformer.[38] Further exposure for a total of 240 s increases the

https://doi.org/10.1021/acs.langmuir.1c00283
Langmuir 2021, 37, 5540−5547

intensities of both N 1s components. With the intensity of the interfacial N−Si species at 398.8 eV approaching saturation, additional exposure appears to increase only the H-bonded species, which has a lower sticking coefficient than the covalently bonded species on the pristine surface during the early adsorption. It is therefore more difficult to grow the H-bonded transitional layer (second adlayer) than the interfacial layer (first adlayer).

A similar increase in intensity with exposure time is also observed in the corresponding O 1s and C 1s spectra. For the thin film samples, the respective broad O 1s feature, with a large full width at half-maximum (fwhm) of 1.8 eV, is located at 532.6 eV, which is 0.7 eV higher in binding energy and 0.15 eV larger in fwhm than those for the powder sample. The higher binding energy and the larger width suggest that alanine has a neutral COOH group in thin films. The C 1s spectra are fitted with three components at 285.3, 286.5, and 289.2 eV with similar intensities, with the binding energies of the former two components being nearly the same as the corresponding ones of the powder sample. However, the higher binding energy component at 289.2 eV is evidently 0.5 eV higher than that of the powder sample, which is quite apparent with the presence of a deeper valley (corresponding to a larger separation) between this feature and the lower-energy band in the film sample than in the powder sample. Since the C 1s binding energy for the neutral carboxylic acid group (COOH) is higher than that for the carboxylate ($-COO^-$), the C 1s result is consistent with the presence of an intact carboxylic acid group in these thin alanine films.

We are not able to grow a thick alanine film on the 7×7 surface held at room temperature, even after attempting to deposit alanine at a higher effusion cell temperature of 140 °C (i.e., a higher deposition rate) and for a longer exposure time (1920 s). The N 1s spectrum of this "thick" film (Figure 1) shows a stronger H-bond-related N···HO feature with similar intensity to the N−Si feature, and a new weak component attributed to NH_3^+ at 402.0 eV. The latter indicates the emergence of only a small amount of "patchy" islands of zwitterions. Evidently, the alanine zwitterionic layer appears to be unstable on Si(111)7×7 at room temperature, with its desorption energy likely smaller than or comparable to the thermal energy at room temperature. The absence of an alanine zwitterionic thick film has also been reported on other surfaces (Cu, Pd, ZnO),[7,19] and it is indeed the notable difference between alanine and glycine film growth on Si(111)7×7.[4] This difference can be understood by examining the respective crystal structures of alanine and glycine in the solid state. Unlike glycine, which has polymorphic forms that all adopt a "layered" structure,[39,40] alanine is orthorhombic and it adopts an "interlocking" structure.[32] As a layered structure is expected to require less energy to assemble in the physical vapor deposition process (vapor−solid phase transformation) than a more complicated interlocking structure, formation of a zwitterionic thick film is more favorable for glycine than alanine on Si(111)7×7 at room temperature. The existence of the methyl group and its associated steric constraints appear to prevent nucleation and solidification of gaseous alanine molecules, such that the vapor−solid phase transformation to a multilayer film is incomplete at room temperature, leaving the Si surface passivated by a thin film consisting of an interfacial and a transitional adlayers, and patchy islands of limited zwitterionic adlayers.

Figure 2 shows the STM images of alanine molecules deposited on a Si(111)7×7 surface at 125 °C for 10 s. Figure

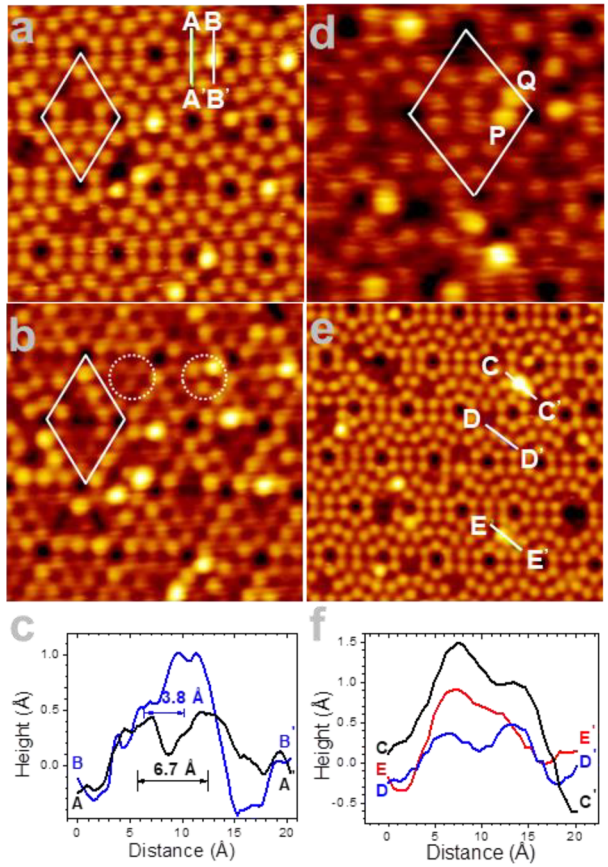

Figure 2. Empty-state (a,d,e) and filled-state (b) STM images of alanine deposited for 10 s on Si(111)7×7 held at room temperature with respective sample bias voltages of +2.4 V and −2.4 V, and both with a tunneling current of 0.2 nA. Images (a) and (b) are collected over the same scanning area of 10.5 nm×10.5 nm. The scan areas for the empty-state images of other selected regions are (d) 7.5 nm×7.5 nm and (e) 15 nm×15 nm. Apparent height profiles in (c) are obtained along two adjacent adatoms across the dimer wall without [line AA′ in (a)] and with adspecies [line BB′ in (a)]. The apparent height profiles along lines CC′, DD′, and EE′ in (e) are shown in (f).

2a,b compare the empty-state and filled-state images of the same scanning area. Evidently, there are additional round protrusions in both empty-state and filled-state images that are bigger and brighter than protrusions corresponding to the Si adatoms. Furthermore, the number of these bright protrusions increases with increasing exposure time (not shown). They can therefore be attributed to a dehydrogenated alanine adspecies, resulting from N−H dissociative adsorption as supported by our XPS results. The bright round protrusion also exhibits a bias dependence in both filled-state and empty-state images, and it becomes invisible when the magnitude of the sample bias is set below 2 V. A closer examination of the empty-state image in Figure 2a shows that the bright round protrusion is not located exactly on top of a Si adatom, but rather off-center from the adatom and gravitating toward the opposite Si adatom across the dimer wall. From the apparent height profiles shown in Figure 2c, the separation between the bright protrusion and the opposite Si adatom across the dimer wall is only 3.8 Å (along line BB′), much smaller than that between

https://doi.org/10.1021/acs.langmuir.1c00283
Langmuir 2021, 37, 5540−5547

two adjacent (unoccupied) Si adatoms across the dimer wall (6.7 Å, along line AA′). Furthermore, the apparent height of the bright protrusion (1.0 Å) is twice that of a Si adatom (0.5 Å). In the filled-state image (Figure 2b), in which the restatoms are clearly visible, the dehydrogenated alanine moieties appear similarly as off-center bright round protrusions as in the empty-state image (Figure 2a). More importantly, the restatom adjacent to the bright round protrusion appears to be absent, while the two other Si adatoms surrounding the missing restatom become concomitantly brighter (marked by a circle on the right, Figure 2b), when compared with the corresponding adatoms without any adspecies (marked by a circle on the left, Figure 2b). These changes in appearance are characteristic of adsorption of a H atom on a restatom. The missing restatom is caused by saturation of the dangling bond (by the H atom), while the reverse charge transfer from the restatom to the surrounding adatoms causes these other two neighboring Si adatoms to appear brighter.[41−43] These STM images therefore provide direct support for N−H dissociative adsorption of an alanine molecule on an adjacent Si adatom−restatom pair, in which the dehydrogenated alanine moiety is bonded to the Si adatom while the dissociated H atom is attached to the nearest restatom. Geometrically, it is more favorable for the larger dehydrogenated alanine moiety to attach to the topmost Si adatom, and for the single small H atom to attach to a restatom, which is 0.8 Å lower than the three surrounding Si adatoms in our DFT calculation.

The discernible minor shift of the dehydrogenated alanine moiety toward the opposite Si adatom across the dimer wall is indicative of a long-range interaction between the unattached carboxylic acid group and the nearest Si adatom across the dimer wall, the latter of which appears hardly changed. Since the hydroxyl group is available for hydrogen bonding (N···HO), as supported by our XPS results, this long-range interaction likely corresponds to the attractive electrostatic interaction between the electron-rich carbonyl O atom and the electron-deficient Si adatom. The discernible minor shift of the dehydrogenated alanine moiety toward the opposite Si adatom across the dimer wall rather than other adatoms or restatoms is the result of the availability of the nearest neighbor bonding site. For a Si adatom on the 7×7 surface, the nearest, second nearest and third nearest neighbors are the restatom (with a separation of 4.6 Å), the opposite adatom across the dimer wall (6.7 Å), and the nearest adatom in the same half unit cell (7.7 Å), respectively.[27] As the restatom (the nearest neighbor) is occupied by the dissociated H atom, the opposite adatom across the dimer wall (the second nearest neighbor) becomes the most favorable site with which the dehydrogenated alanine moiety (already anchored to the adatom site) could interact. Since there are only three restatoms in a 7×7 half unit cell, a half unit cell could accommodate the dissociative adsorption of at most three alanine molecules. When a Si adatom is occupied by a dehydrogenated alanine moiety, it would be of particular interest (in order to understand the early stage in the film growth of alanine) to find out (a) how another alanine molecule would react with the unoccupied opposite Si adatom across the dimer wall, which is no longer pristine due to the adsorbed alanine moiety only 3.8 Å away, and (b) how these two neighboring alanine adspecies interact with each other. The dissociative reaction of this incoming alanine molecule with the adatom-restatom pair is expected to proceed normally because of the availability of unsaturated dangling bonds at these sites. However, the orientation of this newly formed dehydrogenated alanine moiety might be affected by the dehydrogenated alanine adspecies already present across the dimer wall. Thermodynamically, it would be more favorable for these two dehydrogenated alanine to form a dimer via a head-to-head double hydrogen bonding (O···HO and OH···O) arrangement, which has been reported to be responsible for self-assembly of adsorbates containing a carboxylic acid group on inert surfaces.[44,45] While it is difficult to identify the presence of the head-to-head double hydrogen bonding by XPS, given that the O 1s peak is inherently broad and thus not too discriminative, the occurrence of the double hydrogen bonding could perhaps be revealed by the reduced separation between two bright protrusions in STM images. Figure 2d displays two bright protrusions (marked by P and Q) corresponding to dehydrogenated alanine moieties occupying a pair of corner Si adatoms across the dimer wall, with P leaning toward Q and Q leaning toward its opposite Si adatom outside of the marked unit cell. This shift is similar to that depicted in Figure 2a, leading to the off-center characteristic of the protrusion. It is therefore clear that these two dehydrogenated alanine moieties do not shift toward each other, which supports the absence of head-to-head double hydrogen bonding between two dehydrogenated alanine moieties. The lack of the hydrogen bonding formation between two dehydrogenated alanine adspecies could be due to the limited degree of freedom in reorientating the COOH group (to mate with the COOH group from the other dehydrogenated alanine) once a dehydrogenated alanine is anchored by the strong N−Si bonding on the 7×7 surface.

As a bifunctional molecule, alanine has several plausible stable adsorption bonding configurations on Si(111)7×7. The molecule-resolved STM images help to rule out some of the possible bonding configurations. For example, two types of bidentate bonding configurations, in which both the N atom and hydroxyl O atom (following the respective N−H and O−H dissociative adsorption) could bond to either an adjacent adatom-restatom pair or an adatom−adatom pair across the dimer wall, have been found by DFT calculations to be thermodynamically stable for glycine (on adjacent adatom-restatom pair) and glycylglycine (on an adatom−adatom pair across the dimer wall) on the 7×7 surface.[21] As the dehydrogenated alanine protrusion is found to be off-center from a Si adatom and gravitating toward the opposite adatom across the dimer wall, the bidentate bonding configuration on an adjacent adatom-restatom pair can therefore be ruled out, otherwise the protrusion would be located between the adatom and restatom. Furthermore, the essentially unchanged appearance of the opposite adatom across the dimer wall does not support the bidentate bonding configuration on a Si adatom pair across the dimer wall either. Our STM images are therefore more consistent with the monodentate bonding configuration instead of the bidentate adsorption configuration.

Our XPS results also indicate that buildup of alanine molecules in the second adlayer has already begun before completion of the first adlayer, and these second-adlayer molecules bind to dehydrogenated alanine in the first adlayer through the formation of the N···HO hydrogen bond. Figure 2e shows the STM image of one such arrangement of a H-bonded alanine molecule on top of a dehydrogenated alanine moiety (but over the other half unit cell), even at a low coverage. It should be noted that it is generally challenging to image a surface with a high coverage of organic molecules,

https://doi.org/10.1021/acs.langmuir.1c00283
Langmuir 2021, 37, 5540−5547

because the tip could easily be contaminated and/or the tunneling current could become too small, thus causing the scanning to become unstable. In the apparent height profile along line CC′ shown in Figure 2f, the second-adlayer H-bonded alanine molecule appears brighter than the dehydrogenated alanine in the first adlayer because it is located at a larger height. This H-bonded alanine molecule (the larger brighter protrusion) is evidently connected to a dehydrogenated alanine (the smaller bright protrusion) on the side where the free OH group of the dehydrogenated alanine is expected to be located. Figure 2f also compares two other apparent height profiles obtained across a bare Si adatom−adatom pair across the dimer wall (line DD′), and across a dehydrogenated alanine and the opposite Si adatom across the dimer wall (line EE′), with that for two alanine moieties in two adlayers (line CC′). The apparent heights of the Si adatom, dehydrogenated alanine, and second-adlayer H-bonded alanine molecule are found to be 0.5, 1.0, and 1.5 Å, respectively. These apparent height profiles therefore show that the apparent height of an alanine molecule is 0.5 Å. Furthermore, the lateral separations between the bare Si adatom−adatom pair across the dimer wall, between a dehydrogenated alanine and the opposite Si adatom across the dimer wall, and between two alanine moieties in two adlayers are measured to be 6.7, 3.8, and 6.0 Å, respectively. Apparently, the measured LDOS separation between the two H-bonded alanine in two adlayers (6.0 Å) is much larger than that between a dehydrogenated alanine and its covalently bonded Si adatom (2.9 Å = 6.7 Å − 3.8 Å), in good accord with a shorter bond length for covalent bonding in the latter than that for hydrogen bonding in the former. The appearance of the H-bonded alanine molecule is very stable during scanning, without any fuzzy lines (or streaks), which suggests that the disturbance of the scanning tip has little effect on the alanine molecule (in the second adlayer) attached by hydrogen bonding to the dehydrogenated alanine in the first adlayer.

For the DFT calculation, we first compare the adsorption energies of two monodentate bonding configurations with N−Si and O−Si bonding, following N−H dissociation of an amino group and O−H dissociation of a carboxylic acid group, respectively, on a Si adatom-restatom pair. Figure 3a,b show the top and side views of equilibrium geometries of a dehydrogenated alanine molecule adsorbed on a center Si adatom in a faulted half unit cell through the respective O−Si and N−Si bonding, with the corresponding dissociated H atom attached on the nearest Si restatom site. Surprisingly, in contrast to the experimental results, where N−Si covalent bonding is detected by XPS, the calculated results reveal a more stable adsorption configuration through O−Si bonding (with an adsorption energy of −2.40 eV) than that through N−Si bonding (with an adsorption energy of −2.16 eV). The monodentate O−Si bonding configuration is therefore 0.24 eV more thermodynamically stable than the N−Si bonding configuration. As the DFT calculation only provides the equilibrium bonding configurations with local, not global, free energy minima of plausible bonding configurations without consideration of the details of the reaction process (pathways and intermediates), the most thermodynamically stable bonding configuration does not always preclude other realities because of the presence of energy barriers in the reaction pathways to the final configuration. It is clear that alanine adsorption on Si(111)7×7 is kinetically controlled rather than thermodynamically controlled.

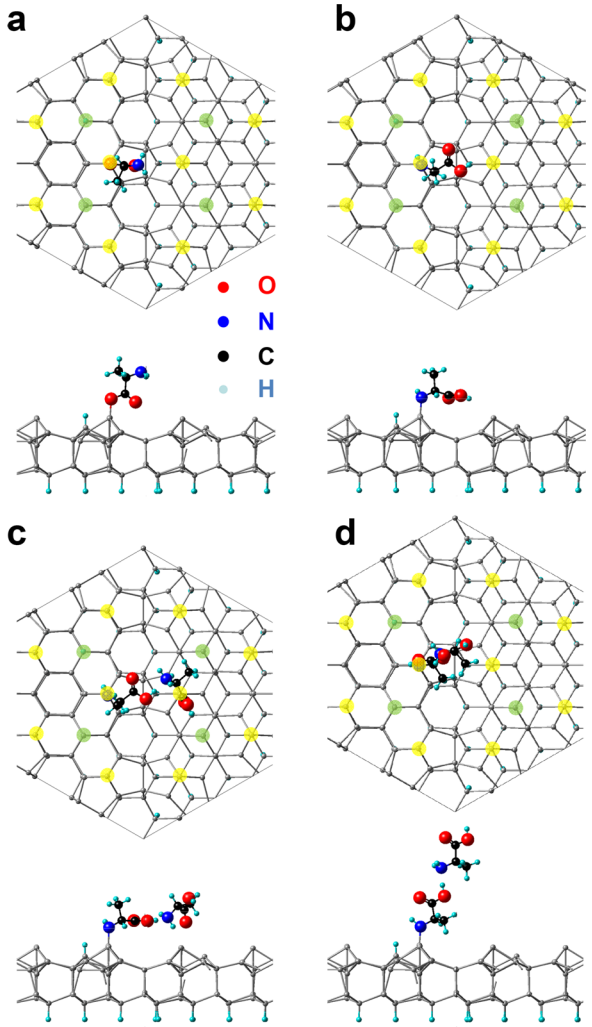

Figure 3. Top and side views of equilibrium geometries of monodentate adsorption configurations of alanine on a Si adatom-restatom pair, with the dehydrogenated alanine moiety on a center Si adatom and the dissociated H atom on the nearest restatom in a faulted half unit cell, involving (a) O−Si bonding (with an adsorption energy of −2.40 eV), and (b) N−Si bonding (with an adsorption energy of −2.16 eV). Top and side views of equilibrium geometries of the dehydrogenated alanine moiety shown in (b) bonded to an alanine molecule by N···HO hydrogen bonding (c) near-horizontally (with an adsorption energy of −2.99 eV) and (d) near-vertically (with an adsorption energy of −2.79 eV).

We have also calculated the bonding configurations of an alanine molecule hydrogen-bonded to a dehydrogenated alanine moiety attached to a center Si adatom (in a faulted half unit cell) by N−Si bonding, with the dissociated H atom bonded to a nearby restatom. With the carboxyl group of the dehydrogenated alanine overhanging the dimer wall, the OH group could be positioned in a horizontal, or vertical or tilted orientation to enable N···HO hydrogen bonding with an alanine molecule. We have obtained several plausible bonding configurations, two of which are shown in Figure 3c,d. In the most stable configuration with an adsorption energy of −2.99 eV (Figure 3c), the carboxyl group of the dehydrogenated alanine is essentially parallel to the 7×7 surface, whereas the hydrogen-bonded alanine molecule is overhanging on the edge of the unfaulted half unit cell. This is consistent with what we observe in the STM image (Figure 2e). On the other hand,

https://doi.org/10.1021/acs.langmuir.1c00283
Langmuir 2021, 37, 5540−5547

when the hydroxyl group of the dehydrogenated alanine is vertical to the 7×7 surface (Figure 3d), the hydrogen bonded alanine molecule is far above the dimer wall. The resulting near-vertical configuration has an adsorption energy of −2.79 eV and is less stable than the horizontal bonding configuration shown in Figure 3c. Furthermore, we have also tried placing an alanine zwitterion on top of the hydrogen-bonded alanine molecule shown in Figure 3c. However, energy minimization has led to a bonding configuration where this zwitterion forms a chemical bonding with a nearby unoccupied Si adatom. This therefore provides indirect support for the lack of alanine zwitterionic thick film formation.

CONCLUSION

We have investigated the adsorption and film growth of alanine on Si(111)7×7 by combining our XPS and STM results with DFT calculations. Our XPS results indicate that alanine undergoes N−H dissociative adsorption on Si(111)7×7 by N−H bond cleavage followed by N−Si bond formation. Furthermore, a second (transitional) alanine adlayer binds to the first (interfacial) adlayer by N···HO hydrogen bonding. In contrast to glycine adsorption on Si(111)7×7, no thick zwitterionic alanine film is observed. Remarkably, the observed interfacial N−H dissociative adsorption is found in the DFT calculation to be less thermodynamically stable than O−H dissociative adsorption, suggesting that the experimentally detected reaction is kinetically, rather than thermodynamically, controlled. In our STM images, a dehydrogenated alanine moiety appears as a bright round protrusion, in registry with a Si adatom, but slightly off-center from the Si adatom and gravitating toward the opposite Si adatom across the dimer wall. Occupation of the adjacent restatom by the dissociated H atom is revealed in the filled-state images. These XPS and STM results provide strong evidence for the aforementioned N−H dissociative adsorption configuration. Furthermore, the carbonyl O atom of the dehydrogenated alanine moiety appears to interact electrostatically with the opposite Si adatom across the dimer wall, which gives rise to its off-center character in our STM image. The position of the dehydrogenated alanine and the appearance of surrounding Si adatoms also help to rule out other plausible bonding configurations, such as bidentate configurations involving N and O atoms bonded to a Si adatom-restatom pair, or to Si adatom−adatom across the dimer wall. An H-bonded second-adlayer alanine molecule has been observed as a brighter and larger protrusion in the half unit cell other than where the dehydrogenated first-adlayer alanine is located. Such geometric arrangement of the two alanine in two adlayers is found to be more stable among several other plausible arrangements as revealed in our DFT calculations. We have therefore demonstrated the power of combining XPS and STM data with DFT calculations in providing insights into the adsorption of amino acids on Si(111)7×7 at the molecular level.

AUTHOR INFORMATION

Corresponding Author

K. T. Leung − *WATLab, and Department of Chemistry, University of Waterloo, Waterloo, Ontario, Canada N2L 3G1*; orcid.org/0000-0002-1879-2806; Email: tong@uwaterloo.ca

Authors

L. Zhang − *WATLab, and Department of Chemistry, University of Waterloo, Waterloo, Ontario, Canada N2L 3G1*

H. Farkhondeh − *WATLab, and Department of Chemistry, University of Waterloo, Waterloo, Ontario, Canada N2L 3G1*; orcid.org/0000-0001-6670-3452

F. R. Rahsepar − *WATLab, and Department of Chemistry, University of Waterloo, Waterloo, Ontario, Canada N2L 3G1*; orcid.org/0000-0003-2359-2523

A. Chatterjee − *WATLab, and Department of Chemistry, University of Waterloo, Waterloo, Ontario, Canada N2L 3G1*

Complete contact information is available at: https://pubs.acs.org/10.1021/acs.langmuir.1c00283

Notes

The authors declare no competing financial interest.

ACKNOWLEDGMENTS

This work was supported by the Natural Sciences and Engineering Research Council of Canada.

REFERENCES

(1) Hamers, R. J. Formation and Characterization of Organic Monolayers on Semiconductor Surfaces. *Annu. Rev. Anal. Chem.* **2008**, *1*, 707−736.

(2) Mirkin, C. A.; Taton, T. A. Semiconductors meet biology. *Nature* **2000**, *405*, 626−627.

(3) Barlow, S. M.; Raval, R. Complex organic molecules at metal surfaces: bonding, organisation and chirality. *Surf. Sci. Rep.* **2003**, *50*, 201−341.

(4) Zhang, L.; Chatterjee, A.; Ebrahimi, M.; Leung, K. T. Hydrogen-bond mediated transitional adlayer of glycine on Si(111)7×7 at room temperature. *J. Chem. Phys.* **2009**, *130*, 121103.

(5) Chatterjee, A.; Zhang, L.; Leung, K. T. Direct Imaging of Hydrogen Bond Formation in Dissociative Adsorption of Glycine on Si(111)7×7 by Scanning Tunneling Microscopy. *J. Phys. Chem. C* **2012**, *116*, 10968−10975.

(6) Jones, G.; Jones, L. B.; Thibault-Starzyk, F.; Seddon, E. A.; Raval, R.; Jenkins, S. J.; Held, G. The local adsorption geometry and electronic structure of alanine on Cu{110}. *Surf. Sci.* **2006**, *600*, 1924−1935.

(7) Gao, F.; Li, Z. J.; Wang, Y.; Burkholder, L.; Tysoe, W. T. Chemistry of Alanine on Pd(111): Temperature-programmed desorption and X-ray photoelectron spectroscopic study. *Surf. Sci.* **2007**, *601*, 3276−3288.

(8) Barlow, S. M.; Louafi, S.; Le Roux, D.; Williams, J.; Muryn, C.; Haq, S.; Raval, R. Supramolecular Assembly of Strongly Chemisorbed Size- and Shape-Defined Chiral Clusters: *S*- and *R*-Alanine on Cu(110). *Langmuir* **2004**, *20*, 7171−7176.

(9) Barlow, S. M.; Louafi, S.; Le Roux, D.; Williams, J.; Muryn, C.; Haq, S.; Raval, R. Polymorphism in supramolecular chiral structures of R- and S-alanine on Cu(110). *Surf. Sci.* **2005**, *590*, 243−263.

(10) Haq, S.; Massey, A.; Moslemzadeh, N.; Robin, A.; Barlow, S. M.; Raval, R. Racemic versus Enantiopure Alanine on Cu(110): An Experimental Study. *Langmuir* **2007**, *23*, 10694−10700.

(11) Iwai, H.; Egawa, C. Molecular Orientation and Intermolecular Interaction in Alanine on Cu(001). *Langmuir* **2010**, *26*, 2294−2300.

(12) Zhao, X. Y.; Zhao, R. G.; Yang, W. S. Adsorption of alanine on Cu(001) studied by scanning tunneling microscopy. *Surf. Sci.* **1999**, *442*, L995−L1000.

(13) Quevedo, W.; Ontaneda, J.; Large, A.; Seymour, J. M.; Bennett, R. A.; Grau-Crespo, R.; Held, G. Adsorption of Aspartic Acid on Ni{100}: A Combined Experimental and Theoretical Study. *Langmuir* **2020**, *36*, 9399−9411.

(14) Farkhondeh, H.; Rahsepar, F. R.; Zhang, L.; Leung, K. M. Structural and Chemical Evolution of L-Cysteine Nanofilm on Si(111)- $\sqrt{3}\times\sqrt{3}$-Ag: From Preferential Growth at Step Edges and Antiphase Boundaries at Room Temperature to Adsorbate-Mediated Metal Cluster Formation at Elevated Temperature. *Langmuir* **2019**, *35*, 16185−16200.
(15) Farkhondeh, H.; Rahsepar, F. R.; Zhang, L.; Leung, K. T. Aligned Organic Molecular Wires in Methionine Nanofilm Growth on Si(111)-$\sqrt{3}\times\sqrt{3}$-Ag. *J. Phys. Chem. C* **2021**, *125*, 4223−4234.
(16) Humblot, V.; Tielens, F.; Luque, N. B.; Hampartsoumian, H.; Methivier, C.; Pradier, C. M. Characterization of Two-Dimensional Chiral Self-Assemblies L- and D-Methionine on Au(111). *Langmuir* **2014**, *30*, 203−212.
(17) Tranca, I.; Smerieri, M.; Savio, L.; Vattuone, L.; Costa, D.; Tielens, F. Unraveling the Self-Assembly of the (S)-Glutamic Acid "Flower" Structure on Ag(100). *Langmuir* **2013**, *29*, 7876−7884.
(18) Seljamae-Green, R. T.; Simpson, G. J.; Grillo, F.; Greenwood, J.; Francis, S. M.; Schaub, R.; Lacovig, P.; Baddeley, C. J. Assembly of a Chiral Amino Acid on an Unreactive Surface: (S)-Proline on Au(111). *Langmuir* **2014**, *30*, 3495−3501.
(19) Gao, Y. K.; Traeger, F.; Shekhah, O.; Idriss, H.; Wöll, C. Probing the interaction of the amino acid alanine with the surface of ZnO($10\bar{1}0$). *J. Colloid Interface Sci.* **2009**, *338*, 16−21.
(20) Ardalan, P.; Davani, N.; Musgrave, C. B. Attachment of Alanine and Arginine to the Ge(100)-2×1 Surface. *J. Phys. Chem. C* **2007**, *111*, 3692−3699.
(21) Zhang, L.; Chatterjee, A.; Leung, K. T. Three-Stage Growth of Glycine and Glycylglycine Nanofilms on Si(111)7×7 and Their Thermal Evolution in Ultrahigh Vacuum Condition: From Chemisorbed Adstructures to Transitional Adlayer to Zwitterionic Films. *J. Phys. Chem. C* **2011**, *115*, 14155−14163.
(22) Rahsepar, F. R.; Zhang, L.; Farkhondeh, H.; Leung, K. T. Biofunctionalization of Si(111)7×7 by "Renewable" L-Cysteine Transitional Layer. *J. Am. Chem. Soc.* **2014**, *136*, 16909−16918.
(23) Rahsepar, F. R.; Leung, K. T. Surface Functionalization of Reconstructed Si(111) with Methionine. *J. Phys. Chem. C* **2019**, *123*, 26980−26988.
(24) Takayanagi, K.; Tanishiro, Y.; Takahashi, M.; Takahashi, S. Structural analysis of Si(111)-7×7 by UHV-transmission electron diffraction and microscopy. *J. Vac. Sci. Technol., A* **1985**, *3*, 1502−1506.
(25) Northrup, J. E. Origin of surface states on Si(111)(7×7). *Phys. Rev. Lett.* **1986**, *57*, 154−157.
(26) Wolkow, R.; Avouris, Ph. Atom-resolved surface chemistry using scanning tunneling microscopy. *Phys. Rev. Lett.* **1988**, *60*, 1049−1052.
(27) Tao, F.; Xu, G. Q. Attachment Chemistry of Organic Molecules on Si(111)-7×7. *Acc. Chem. Res.* **2004**, *37*, 882−893.
(28) Blöchl, P. E.; Jepsen, O.; Andersen, O. K. Improved tetrahedron method for Brillouin-zone integrations. *Phys. Rev. B: Condens. Matter Mater. Phys.* **1994**, *49*, 16223−16233.
(29) Kresse, G.; Joubert, D. From ultrasoft pseudopotentials to the projector augmented-wave method. *Phys. Rev. B: Condens. Matter Mater. Phys.* **1999**, *59*, 1758−1775.
(30) Perdew, J. P.; Burke, K.; Ernzerhof, M. Generalized Gradient Approximation Made Simple. *Phys. Rev. Lett.* **1996**, *77*, 3865−3868.
(31) Grimme, S. Semiempirical GGA-type density functional constructed with a long-range dispersion correction. *J. Comput. Chem.* **2006**, *27*, 1787−1799.
(32) Tulip, P. R.; Clark, S. J. Structural and electronic properties of L-amino acids. *Phys. Rev. B: Condens. Matter Mater. Phys.* **2005**, *71*, 195117.
(33) Clark, D. T.; Peeling, J.; Colling, L. An experimental and theoretical investigation of the core level spectra of a series of amino acids, dipeptides and polypeptides. *Biochim. Biophys. Acta, Protein Struct.* **1976**, *453*, 533−545.
(34) Zhao, X. Y.; Rodriguez, J. Photoemission study of glycine adsorption on Cu/Au(1 1 1) interfaces. *Surf. Sci.* **2006**, *600*, 2113−2121.
(35) Cao, X. P.; Hamers, R. J. Silicon Surfaces as Electron Acceptors: Dative Bonding of Amines with Si(001) and Si(111) Surfaces. *J. Am. Chem. Soc.* **2001**, *123*, 10988−10996.
(36) Cao, X. P.; Coulter, S. K.; Ellison, M. D.; Liu, H. B.; Liu, J. M.; Hamers, R. J. Bonding of Nitrogen-Containing Organic Molecules to the Silicon(001) Surface: The Role of Aromaticity. *J. Phys. Chem. B* **2001**, *105*, 3759−3768.
(37) Zhang, L.; Chatterjee, A.; Leung, K. T. Hydrogen-Bond-Mediated Biomolecular Trapping: Reversible Catch-and-Release Process of Common Biomolecules on a Glycine-Functionalized Si(111)7×7 Surface. *J. Phys. Chem. Lett.* **2010**, *1*, 3385−3390.
(38) Feyer, V.; Plekan, O.; Richter, R.; Coreno, M.; Prince, K. C.; Carravetta, V. Core Level Study of Alanine and Threonine. *J. Phys. Chem. A* **2008**, *112*, 7806−7815.
(39) Iitaka, Y. Crystal Structure of β-Glycine. *Nature* **1959**, *183*, 390−391.
(40) Iitaka, Y. The Crystal Structure of β -Glycine. *Acta Crystallogr.* **1960**, *13*, 35−45.
(41) Lo, R. L.; Hwang, I. S.; Ho, M. S.; Tsong, T. T. Diffusion of Single Hydrogen Atoms on Si(111)-(7×7) Surfaces. *Phys. Rev. Lett.* **1998**, *80*, 5584−5587.
(42) Lo, R. L.; Hwang, I. S.; Tsong, T. T. Complete dissociation of water on hot silicon (111)−7×7 surface−−direct observation of hopping oxygen atom. *Surf. Sci.* **2003**, *530*, L302−L306.
(43) Vittadini, A.; Selloni, A. Binding Sites, Migration Paths, and Barriers for Hydrogen on Si(111)-(7×7). *Phys. Rev. Lett.* **1995**, *75*, 4756−4759.
(44) Payer, D.; Comisso, A.; Dmitriev, A.; Strunskus, T.; Lin, N.; Wöll, C.; DeVita, A.; Barth, J. V.; Kern, K. Ionic Hydrogen Bonds Controlling Two-Dimensional Supramolecular Systems at a Metal Surface. *Chem. - Eur. J.* **2007**, *13*, 3900−3906.
(45) Kuehnle, A.; Linderoth, T. R.; Hammer, B.; Besenbacher, F. Chiral recognition in dimerization of adsorbed cysteine observed by scanning tunnelling microscopy. *Nature* **2002**, *415*, 891−893.

https://doi.org/10.1021/acs.langmuir.1c00283
Langmuir 2021, 37, 5540−5547